JACS
JOURNAL OF THE AMERICAN CHEMICAL SOCIETY

COMMUNICATION

pubs.acs.org/JACS

Self-Assembling Small Molecules Form Nanofibrils That Bind Procaspase-3 To Promote Activation

Julie A. Zorn,[†] Holger Wille,[‡,§] Dennis W. Wolan,[†,⊥] and James A. Wells*[,†,∥]

[†]Department of Pharmaceutical Chemistry, [‡]Institute for Neurodegenerative Disease, [§]Department of Neurology, and [∥]Department of Cellular and Molecular Pharmacology, University of California, San Francisco, California

Supporting Information

ABSTRACT: Modulating enzyme function with small-molecule activators, as opposed to inhibitors, offers new opportunities for drug discovery and allosteric regulation. We previously identified a compound, called 1541, from a high-throughput screen (HTS) that stimulates activation of a proenzyme, procaspase-3, to generate mature caspase-3. Here we further investigate the mechanism of activation and report the surprising finding that 1541 self-assembles into nanofibrils exceeding 1 μm in length. These particles are an unanticipated outcome from an HTS that have properties distinct from standard globular protein aggregators. Moreover, 1541 nanofibrils function as a unique biocatalytic material that activates procaspase-3 via induced proximity. These studies demonstrate a novel approach for proenzyme activation through binding to fibrils, which may mimic how procaspases are naturally processed on protein scaffolds.

Many proteases are expressed in dormant forms, known as zymogens, that are activated in response to diverse stimuli. Activation of these latent enzymes is often catalyzed by processing from upstream proteases and, in some cases, via autoproteoylsis.[1] These transitions can be promoted by binding cofactors, sequestering cellular inhibitors, or interacting with signaling complexes.[2] Cysteine aspartyl proteases (caspases) are expressed as such inactive precursors, or procaspases, which become activated in fate-determining transformations as diverse as cell death, innate immune responses, and differentiation.[3] Further mechanistic insight into the processes that facilitate procaspase activation will foster the design of novel chemical probes to study the sufficiency of caspases for these phenotypes.[4,5]

Procaspases are typically activated upon cleavage by upstream proteases or binding to protein scaffolds in response to intrinsic or extrinsic cellular signals.[6] For example, the apoptosome recruits procaspase-9, the death-inducing signaling complex (DISC) interacts with procaspase-8, and the various inflammasome complexes associate with procaspase-1 to stimulate activity.[3,7] Procaspases bind to these signaling platforms, which triggers clustering, oligomerization and/or a conformation change, and proteolytic processing. Removal of an N-terminal prodomain and an additional cleavage to yield a large and small subunit generate the mature enzyme.[8] While procaspase-3 self-activation is normally restricted under physiological conditions, autoproteolysis can occur.[9]

In an earlier investigation, we identified a synthetic small molecule, termed 1541 (Chart 1), that promotes autoactivation of procaspase-3.[10] After a lag phase, the compound induces a burst in activity due to the formation of processed caspase-3. These results plus additional characterization suggest that the compounds work through an allosteric mechanism to promote autoproteolysis. In this study, we show that 1541 and related analogues spontaneously assemble into highly ordered nanofibrils. Procaspase-3 becomes immobilized on the surface of the fibrils and generates active caspase-3. It is conceivable that these "amyloid-like" fibrils mimic natural protein scaffolds for activating procaspases.

Chart 1. Compound 1541 and Analogues

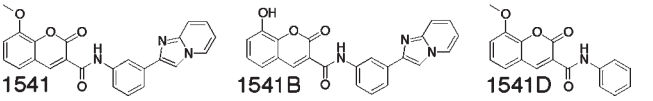

Globular aggregates of small molecules that inhibit enzyme activity have been described previously.[11−13] These aggregates are readily identified by diagnostic experiments, including detergent sensitivity, β-lactamase inhibition, and sensitivity to bovine serum albumin (BSA).[14−16] Furthermore, others have reported that detergent-sensitive molecules in screening libraries can also promote enzyme activity.[17] We performed these diagnostic tests on 1541 with mixed results. For example, common detergents such as Triton or CHAPS did not disrupt procaspase-3 activation, and 1541 did not inhibit β-lactamase (Figures S1 and S2 in the Supporting Information). Unexpectedly, the addition of BSA protected against procaspase-3 activation (Figure S3). This result alone is not definitive, since BSA contains hydrophobic patches that can bind soluble small molecules.

Because of these inconclusive results, we investigated the solubility of 1541 by centrifugation.[18] Surprisingly, 1541 pelleted from solution at 16100g with a solubility constant (K_{sp}) of 1−2 μM, concentrations close to the concentration of half-maximal activation (AC_{50}) of procaspase-3 by 1541 (Figure 1A and Figure S1). Interestingly, both active and inactive analogues pelleted upon centrifugation, suggesting that the particles may not necessarily be responsible for the observed activity (Figure S4).

We next evaluated whether procaspase-3 could directly interact with the particulates. We used procaspase-3 (C163A), an inactive/catalytically dead variant, to analyze the binding directly without the complication of processing. Varying concentrations of 1541 and 1541B were added to 200 nM procaspase-3 (C163A). The solutions were immediately centrifuged, and the amounts of procaspase-3 in the pellet were assayed by gel electrophoresis and quantified by densitometry (Figure S4). We observed cosedimentation of the C163A enzyme for both 1541 and 1541B at concentrations that correlated to their AC_{50} values (Figure 1B and Figure S5). Furthermore, enzyme

Received: September 4, 2011
Published: November 08, 2011

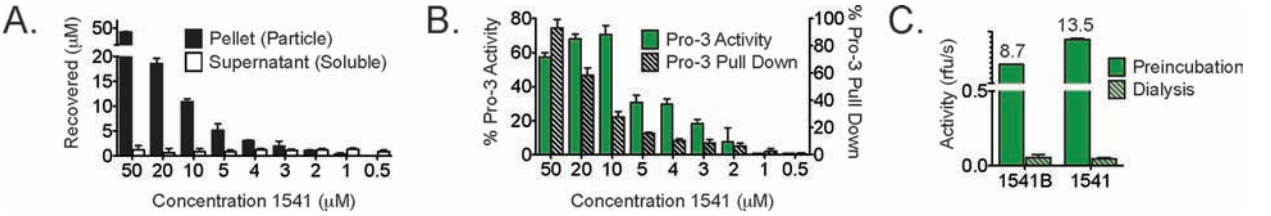

Figure 1. 1541 forms particles that are required for binding and activation of procaspase-3. (A) The amounts of 1541 in the pellet (solid black bars) and the supernatant (open bars) were analyzed after centrifugation. (B) (i) Samples of procaspase-3 (C163A) with varying concentrations of 1541 were centrifuged, and the amount of procaspase-3 in the pellet was determined (hatched bars). (ii) The activity of wild-type procaspase-3 with 1541 was determined (filled green bars). (C) In a preincubation control sample, procaspase-3 was added to 10 μM 1541 (or 1541B) inside a dialysis membrane (filled green bars). In the test sample, only procaspase-3 was inside the dialysis chamber, with 1541 (or 1541B) outside the chamber (hatched green bars). After 12 h at 37 °C, the activity of each sample was measured.

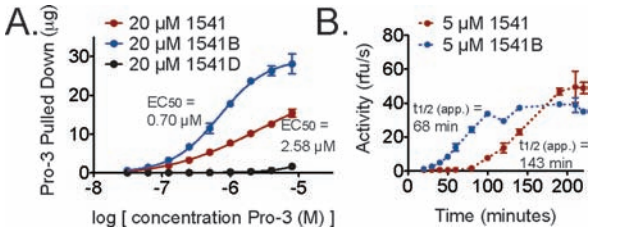

Figure 2. 1541 and 1541B particles have different affinities for procaspase-3 that correlate to distinct rates of activation. (A) 1541, 1541B, or 1541D (20 μM) was incubated with a dilution series of procaspase-3 (C163A). After centrifugation, the pellet was examined for procaspase-3. (B) 1541 or 1541B (5 μM) was added to wild-type procaspase-3, and activities were plotted versus time. An apparent $t_{1/2}$ value incorporating the lag phase and the actual $t_{1/2}$ value were calculated for each compound. Notably, the distinct lag phases drive the difference in the apparent $t_{1/2}$ values.

sedimentation was not observed with the inactive analogue 1541D, even though compound sedimentation occurred. These data provide evidence that procaspase-3 binds to the high-molecular-weight particulates of the active compounds. While the data suggest a mechanism dependent on particles, both soluble small molecules and larger particles were present in the activation assay.

We performed a dialysis experiment to establish the relevant activating species. Procaspase-3 was placed inside a dialysis chamber with a 12−14 kDa molecular weight cutoff (~2 nm radius of gyration), and 10 μM 1541 or 1541B was placed in buffer outside the membrane. After a 12 h incubation, no activation or processing of the proenzyme was observed (Figure 1C and Figure S6). In contrast, when the compounds were placed both inside and outside of the dialysis membrane, we saw dramatic activation and complete processing of procaspase-3. This suggests that particulates larger than roughly 4 nm are responsible for the activation effects.

We subsequently analyzed if 1541 and 1541B particles exhibit saturation behavior to assess whether the compounds provide a fixed number of binding sites to accommodate the enzyme or promote nonspecific aggregation of procaspase-3. We set the concentration of the active analogues at 20 μM, 10-fold above their K_{sp} values, and titrated them with procaspase-3 (C163A) to investigate binding saturation directly. The mixtures were centrifuged, and the amounts of enzyme in the pellets were measured. The particulates from both compounds showed clear saturation behavior, yet with varying affinities for procaspase-3 (Figure 2A and Figure S7). Furthermore, when monitoring the rates of procaspase-3 activation by 1541 and 1541B, we found that the binding affinity and activation rate were coincident (Figure 2B). This suggests that procaspase-3 is immobilized by the particles with specific and saturable sites of interaction that impact the activity.

While the particles of 1541 and 1541B seemed to account for procaspase-3 activation, they were resistant to standard tests of small-molecule aggregation. Thus, we determined whether compounds that are known to form aggregates could activate procaspase-3.[11,16] Six aggregators that are well-known for promiscuous enzyme inhibition were incapable of activating procaspase-3 (Figure S8). We did see that one of the promiscuous compounds, Congo red, inhibited mature caspase-3. As expected, the inhibition of caspase-3 by the aggregator was detergent-sensitive (Figure S8). This demonstrated a functional interaction between Congo red and caspase-3, but no activation of procaspase-3 was observed. In contrast, 1541 particles appear to be responsible for procaspase-3 activation and behave differently from standard aggregators. Because of the discrepancies in behavior, we sought to characterize further the physical properties of 1541 to establish whether it exhibits novel properties of known colloidal aggregators or assembles into unique particles that promote procaspase-3 activity.

As with the centrifugation experiments, dynamic light scattering (DLS) studies demonstrated the presence of particles at room temperature for 10 μM 1541 and 1541B. Remarkably, these particles showed characteristics distinct from standard aggregators (Table 1 and Figure S9). Common properties of aggregators have been previously published, with 3′,3″,5′,5″-tetraiodophenolphthalein (TIPT) repeated here for direct comparison.[15,19] The intensities of scattered light (I_{DLS}) for 1541 and 1541B were 10−20-fold lower than for TIPT [270.2, 170.1, and 3903.5 kilocounts/s (kcps), respectively]. Conversely, the radii determined by DLS (r_{DLS}) for 1541 and 1541B particles (1112.8 and 910.7 nm) were >10-fold greater than that of TIPT (71.1 nm). The inactive analogue 1541D had properties similar to TIPT (I_{DLS} = 3317.0 kcps, r_{DLS} = 164.1 nm). These results suggest that 1541 and 1541B form particles that are different from 1541D and other standard colloidal aggregates.

The distinct properties of 1541 and 1541B were further characterized by particle flow cytometry.[18] Notably, the K_{sp} values determined for 1541 and 1541B closely matched the AC_{50} values for self-activation of procaspase-3 (Table 1). The particle counts increased linearly with concentration until reaching maximum values at 4 μM for 1541 and 5 μM for 1541B (Figure S10). Increasing the concentration beyond this point generated only larger particle sizes and not larger numbers of particles. Once nucleated, 1541 and 1541B particles appear to favor recruitment of additional small molecules to grow in size. Conversely, TIPT and 1541D appear to maintain a constant size but increase the particle count with increasing concentration

Table 1. Unique Properties of 1541 and Related Analogues Compared with Standard Aggregators

sample[a]	T (°C)	I_{DLS} (kcps)	r_{DLS} (nm)	K_{sp} (μM)[b]	AC_{50} (μM)[c]
control	25	19.7 ± 1.3	1.0 ± 0.3	no particles	NA
control	37	20.8 ± 1.2	1.3 ± 0.3	no particles	NA
1541	25	270.2 ± 77.9	1112.8 ± 86.6	1.3 ± 0.3	>50
1541	37	17.5 ± 1.4	0.5 ± 0.1	10 ± 5	3.0 ± 0.6
1541B	25	170.1 ± 44.7	910.7 ± 66.7	1.6 ± 0.4	3.1 ± 0.5[d]
1541B	37	15.8 ± 0.9	0.4 ± 0.1	20 ± 5	1.8 ± 0.1
1541D	25	3317.0 ± 854.0[e]	164.1 ± 7.7	7.5 ± 0.5	NA
1541D	37	3071.9 ± 465.1[e]	186.4 ± 21.6	7.5 ± 0.5	NA
TIPT	25	3903.5 ± 1423.0	71.1 ± 8.6	–	NA
TIPT	37	3933.2 ± 1369.0	76.7 ± 7.8	–	NA

[a] Control samples contained no aggregator. The concentrations of 1541, 1541B, and 1541D in DLS measurements were 10 μM. The concentration of TIPT was 50 μM. [b] Determined using particle flow cytometry. [c] Activity measurements were performed at t = 8 h. NA = no activation. [d] The maximum percent activation for 1541B was 8% at 25 °C vs 60% at 37 °C. [e] 1541D samples were run at 25% laser power.

(Figure S10). These results further depict unique features of 1541 and 1541B in comparison with standard aggregators.

Since procaspase-3 self-activation assays are performed at 37 °C, we studied the properties of 1541 and 1541B particles after agitation at this temperature. Interestingly, the I_{DLS} and r_{DLS} values for 1541 and 1541B particles decreased to buffer values for these conditions (Table 1). Because the particle flow cytometer also uses light scattering to detect particles, shifts in K_{sp} to 10 and 20 μM at 37 °C were similarly observed for both 1541 and 1541B, respectively. Nonetheless, incubation and centrifugation of 1541 and 1541B at 37 °C still resulted in pelleting of the compound (Figure S11). These results indicate that the particles were still present at increased temperatures but were significantly altered and became undetectable by light scattering. Notably, temperature had minimal impact on the properties of both TIPT and 1541D.

Given the strong evidence that the particles of 1541 and 1541B are distinct from promiscuous inhibitors, we investigated the molecular structure of 1541 relative to a colloidal aggregator, TIPT, by transmission electron microscopy (TEM). TEM images of TIPT showed the typical globular structures of known aggregators (Figure S12). In dramatic contrast, 1541 produced long thin fibrils extending to over 1 μm in length (Figure 3). The fibrils tended to cluster into braided bundles, but individual strands were as thin as 2.6 nm, perhaps only a few molecules thick (Figure S12). At 37 °C, 1541 tended to form thicker fibrils and typically appeared as single strands rather than the larger tangles observed at room temperature. Consistent with the tangles breaking apart at higher temperatures, we observed delayed centrifugation of 1541 particles after a 1 h incubation at 37 °C (compared with room temperature) (Figure S13). Disrupting the clusters at 37 °C may allow a greater extent of the fibril surface to be accessible to the procaspase to facilitate activation. However, additional experiments are necessary to elucidate the temperature effects.

We subsequently examined whether binding of procaspase-3 to 1541 fibrils could be observed by TEM. We incubated 50 μM 1541 with 500 nM procaspase-3 (C163A) at 37 °C and also at 25 °C. At both temperatures, the edges of the nanofibrils no longer looked crisp but appeared to be decorated with protein particles, suggesting that procaspase-3 lined the length of the

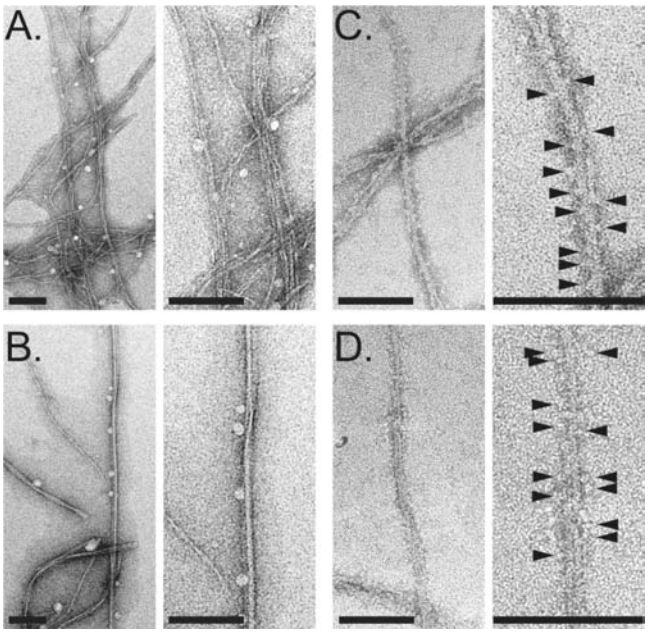

Figure 3. TEM images of 1541 nanofibrils with and without procaspase-3. (A) Negatively stained 1541 at 25 °C shows bundles of very thin and flexible fibrils. (B) In contrast, 1541 at 37 °C consists mainly of larger, less flexible fibrils. (C, D) 1541 fibrils decorated with procaspase-3 at (C) 25 °C and (D) 37 °C. The procaspase-3 molecules decorating the surface are indicated by arrowheads. Scale bars = 100 nm.

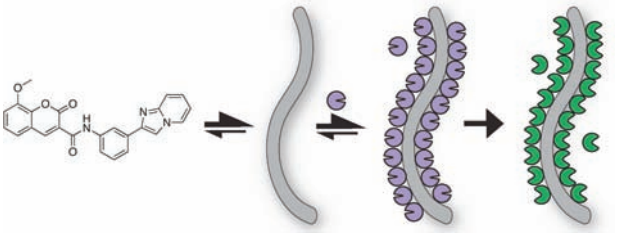

Figure 4. Model of procaspase-3 activation by 1541 nanofibrils. 1541 and analogues spontaneously self-assemble into nanofibrils. The fibrils bind directly to procaspase-3 to promote increased local concentration of the enzyme. Upon recruitment to the fibrils, procaspase-3 is activated to generate mature caspase-3.

fibrils (Figure 3 and Figure S12). The nanofibrils also appeared to be wider, consistent with the enzyme being bound to the surface.

Our results show that 1541 and 1541B spontaneously assemble into nanofibrils that can activate procaspase-3. These particles have properties distinct from those of standard aggregators identified in high-throughput screening, which typically lead to enzyme inhibition.[11] We propose that these fibrils act as a scaffold to concentrate procaspase-3 where it can be processed by other enzymes in close proximity (Figure 4). In this regard, these synthetic fibrils mimic signaling platforms, such as the inflammosomes, the apoptosome, and the DISC, which facilitate procaspase activation.[3,7,20] Alternatively, the fibrils may alter the conformation of the proenzyme to promote intramolecular processing. Further studies are underway to distinguish between cis versus trans activation promoted by the fibrils.

Intriguingly, 1541 particles appear structurally similar to the fibrous β-sheet aggregates formed by amyloid-β proteins (Aβ). Aβ proteins have been shown to facilitate proenzyme activation,

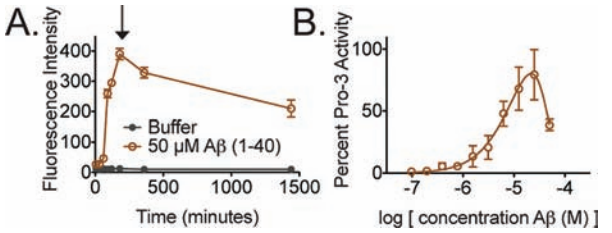

Figure 5. Aβ fibrils activate procaspase-3. (A) Aβ peptide (1−40) was agitated at 37 °C in a caspase activity buffer to form fibrils. Fibril formation was monitored over time by an increase in thioflavin T fluorescence. (B) Aβ peptide (1−40) samples were taken at 3 h (black arrow), serially diluted, and incubated with procaspase-3 for 6 h. Percent activity is shown.

such as the conversion of prekallikrein to kallikrein of the plasma kinin-forming cascade as well as the conversion of plasminogen into the active protease plasmin by the tissue-type plasminogen activator (tPA).[21,22] Furthermore, several cellular proteins assemble into an amyloid fold, such as fibrin and Pmel17, to facilitate natural processes, including proenzyme activation.[23−25] Filamentous structures within the cell have even been shown to associate directly with caspase-3.[26] In this regard, 1541 fibrils appear to mimic endogenous and possibly disease-related fibrous structures on which the procaspases can become concentrated and activated.

To evaluate whether such physiologically relevant fibrils can interact with procaspase-3, we generated fibrils from Aβ (1−40) by agitation of the peptide at 37 °C in a caspase activity buffer (Figure 5A). The Aβ fibrils were subsequently serially diluted and incubated with procaspase-3. Similar to our small-molecule fibrils, addition of these peptide fibrils to procaspase-3 stimulated activation (Figure 5B). This result has potential implications for Alzheimer's disease, where Aβ aggregates have been linked to caspase-dependent neurotoxicity.[27] Moreover, we previously described the apoptotic activity induced by 1541 and 1541B.[10] We are now exploring how these nanofibrils promote cell death. Such a mechanism is certainly intriguing and nonstandard from a drug discovery perspective.

For bioprocessing applications, enzyme immobilization on nanostructures offers an exciting alternative to traditional approaches for manipulating enzyme functionality, such as genetic and chemical engineering.[28,29] 1541 represents a first-in-class, self-assembling, small-molecule nanofibril that acts as a catalyst for procaspase-3 activation. Future studies aim to elucidate the specific structural properties of the molecule that drive fibril assembly as well as those that facilitate procaspase-3 activation. It may be possible to use this scaffold for the design of other proenzyme activators or to discover novel fibril-forming small molecules that activate proenzymes.

■ ASSOCIATED CONTENT

Supporting Information. Supporting figures and detailed experimental procedures. This material is available free of charge via the Internet at http://pubs.acs.org.

■ AUTHOR INFORMATION

Corresponding Author
jim.wells@ucsf.edu

Present Addresses
[⊥]Department of Molecular and Experimental Medicine, The Scripps Research Institute, La Jolla, CA.

■ ACKNOWLEDGMENT

We thank S. Mahrus, N. Agard, and J. Porter for invaluable advice, guidance, and support. We acknowledge M. Bennett and H. Rodriguez at Calithera for advice and discussions. We thank A. Doak, B. Feng, S. Prusiner, and B. Shoichet for helpful discussions on promiscuous enzyme inhibitors and for use of their instruments. We thank D. Hostetter for providing granzyme B. We thank the Wells lab, the Small Molecule Discovery Center at UCSF, and W. F. DeGrado for suggestions. This research was supported by grants from the National Institutes of Health (R01 CA136779, P01 AG02132), a National Cancer Institute Postdoctoral Fellowship (F32 CA119641-03 to D.W.W.), an ARCS Foundation Award (to J.A.Z.), and a Schleroderma Research Foundation Evnin-Wright Fellowship (to J.A.Z.).

■ REFERENCES

(1) Kassell, B.; Kay, J. *Science* **1973**, *180*, 1022.
(2) Turk, B. *Nat. Rev. Drug Discovery* **2006**, *5*, 785.
(3) Li, J.; Yuan, J. *Oncogene* **2008**, *27*, 6194.
(4) Shen, A. *Mol. BioSyst.* **2010**, *6*, 1431.
(5) Zorn, J. A.; Wells, J. A. *Nat. Chem. Biol.* **2010**, *6*, 179.
(6) Salvesen, G. S.; Riedl, S. J. *Adv. Exp. Med. Biol.* **2008**, *615*, 13.
(7) Schroder, K.; Tschopp, J. *Cell* **2010**, *140*, 821.
(8) Stennicke, H. R.; Salvesen, G. S. *Biochim. Biophys. Acta* **2000**, *1477*, 299.
(9) Roy, S.; Bayly, C. I.; Gareau, Y.; Houtzager, V. M.; Kargman, S.; Keen, S. L.; Rowland, K.; Seiden, I. M.; Thornberry, N. A.; Nicholson, D. W. *Proc. Natl. Acad. Sci. U.S.A.* **2001**, *98*, 6132.
(10) Wolan, D. W.; Zorn, J. A.; Gray, D. C.; Wells, J. A. *Science* **2009**, *326*, 853.
(11) McGovern, S. L.; Helfand, B. T.; Feng, B.; Shoichet, B. K. *J. Med. Chem.* **2003**, *46*, 4265.
(12) Ryan, A. J.; Gray, N. M.; Lowe, P. N.; Chung, C.-W. *J. Med. Chem.* **2003**, *46*, 3448.
(13) Reddie, K. G.; Roberts, D. R.; Dore, T. M. *J. Med. Chem.* **2006**, *49*, 4857.
(14) Feng, B. Y.; Simeonov, A.; Jadhav, A.; Babaoglu, K.; Inglese, J.; Shoichet, B. K.; Austin, C. P. *J. Med. Chem.* **2007**, *50*, 2385.
(15) Coan, K. E. D.; Shoichet, B. K. *Mol. BioSyst.* **2007**, *3*, 208.
(16) Seidler, J.; McGovern, S. L.; Doman, T. N.; Shoichet, B. K. *J. Med. Chem.* **2003**, *46*, 4477.
(17) Goode, D. R.; Totten, R. K.; Heeres, J. T.; Hergenrother, P. J. *J. Med. Chem.* **2008**, *51*, 2346.
(18) Coan, K. E. D.; Shoichet, B. K. *J. Am. Chem. Soc.* **2008**, *130*, 9606.
(19) Doak, A. K.; Wille, H.; Prusiner, S. B.; Shoichet, B. K. *J. Med. Chem.* **2010**, *53*, 4259.
(20) Yuan, S.; Yu, X.; Asara, J. M.; Heuser, J. E.; Ludtke, S. J.; Akey, C. W. *Structure* **2011**, *19*, 1084.
(21) Shibayama, Y.; Joseph, K.; Nakazawa, Y.; Ghebreihiwet, B.; Peerschke, E. I.; Kaplan, A. P. *Clin. Immunol.* **1999**, *90*, 89.
(22) Kingston, I. B.; Castro, M. J.; Anderson, S. *Nat. Med.* **1995**, *1*, 138.
(23) Fowler, D. M.; Koulov, A. V.; Alory-Jost, C.; Marks, M. S.; Balch, W. E.; Kelly, J. W. *PLoS Biol.* **2006**, *4*, No. e6.
(24) Kranenburg, O.; Bouma, B.; Kroon-Batenburg, L. M. J.; Reijerkerk, A.; Wu, Y.-P.; Voest, E. E.; Gebbink, M. F. B. G. *Curr. Biol.* **2002**, *12*, 1833.
(25) Fowler, D. M.; Koulov, A. V.; Balch, W. E.; Kelly, J. W. *Trends Biochem. Sci.* **2007**, *32*, 217.
(26) Dinsdale, D.; Lee, J. C.; Dewson, G.; Cohen, G. M.; Peter, M. E. *Am. J. Pathol.* **2004**, *164*, 395.
(27) Wellington, C. L.; Hayden, M. R. *Clin. Genet.* **2000**, *57*, 1.
(28) Kim, J.; Grate, J. W.; Wang, P. *Chem. Eng. Sci.* **2006**, *61*, 1017 .
(29) Ge, J.; Lu, D.; Liu, Z.; Liu, Z. *Biochem. Eng. J.* **2009**, *44*, 53 .